1 eV (1.7 eV) half−Heusler compounds ScAgC, YCuC, CaZnC and NaAgO (LiCuS) lattice-matched to GaAs (Si) for solar cell application: First-principles study

N. Belmiloud[1], F. Boutaiba[1], A. Belabbes[2,3],* M. Ferhat[1], and F. Bechstedt[3]
[1] *Département de Génie Physique, Laboratoire de Physique des Matériaux et Fluides (LPMF), Université des Sciences et de la Technologie d'Oran, USTO, Oran, Algeria*
[2] *King Abdullah University of Science and Technology (KAUST), Thuwal 23955-6900, Saudi Arabia and*
[3] *Institut für Festkörpertheorie und -optik, Friedrich-Schiller-Universität Jena, Max-Wien-Platz 1, 07743 Jena, Germany*

A systematic analysis of 648 half−Heusler compounds [T. Gruhn, Phys. Rev. B **82**, 125210(2010)] is performed to find the appropriate target key physical parameters for photovoltaic application. As a result five ternary half−Heusler compounds ScAgC, YCuC, CaZnC, NaAgO and LiCuS are studied by density functional theory for potential applications in multi−junction solar cells. The calculated formation enthalpies indicate that these materials are thermodynamically stable. Using state−of−the−art modified Becke−Johnson exchange potential approximation, we find a direct band gap close to 1 eV (∼1.88 eV) for ScAgC, YCuC, CaZnC, NaAgO (LiCuS) being quasi−lattice matched to GaAs (Si). In addition, the band offsets between half−Heusler compounds and GaAs (Si) and their consequences for heterostructures are derived using the modified Tersoff method for the branch−point energy. Furthermore, the elastic constants and phonon dispersion curves are calculated. They indicate the respective mechanical and dynamical stability of these half−Heusler compounds.

PACS numbers: 71.15.Mb, 71.15.Mq, 71.20.Nr, 84.60.Jt, 72.40.+w

I. INTRODUCTION

Fossil fuels resources currently supply a large part of the worlds energy needs. Predictions project a picture that a serious depletion will happen with several decades from now. Therefore, finding alternative sources of energy is a vital issue for humanity. The good news is that a significant and promising technology to have emerged out of this quest is the use of solar energy within photovoltaics. This most emission−free energy source is not only renewable, but also clean compared with others energy sources like gas and oil. Basically, the solar cells convert solar power directly into electricity. They are collectively termed as photovoltaic (PV) devices. In the past two decades, high−efficiency multi−junction solar cells have experienced a great expansion due to the increasing power of experimental techniques. Improvements in the epitaxial growth technology, as the metal organic vapor phase epitaxy (MOVPE) and the molecular beam epitaxy (MBE), have opened the way to fabricate promising new materials for PV devices with different design. Among such materials quaternary compounds as GaInNAs[1,2], GaNAsBi[3], GaAsSbN[4,5], (GaInNP)[6,7], and GaNAsP[6–8] have been suggested for application in triple solar cells because of their possible band gap of 1 eV (1.7eV) and the lattice match to GaAs(Si). Unfortunately, due to the large radius mismatch and electronegativity between N and the substituted atoms, the growth of high−quality quaternary alloys is difficult. Both the optical and electrical characteristics are degraded even if only a few percent of N is incorporated because of the compositional fluctuations and phase separation tendency.

Efforts to improve the efficiency of solar cells have led to extensive experimental and theoretical studies of new materials such as the ternaries[9] $CuInSe_2$ and $CuInS_2$, $ZnSnP_2$[10], GaAsP[11], InGaN and InAlN[12], GaNSb[13], or Cu-based quaternaries[14,15] such as the $Cu_2ZnSn(S_4,Se_4)$, $Cu_2Zn(Sn,Ge)Se_4$, $Cu_2Zn(Sn,Si)Se_4$, and GeSiSn alloys lattice−matched to Ge[16]. In this respect also the half−Heusler (hH) compounds are very interesting, since they comprise promising candidates for high−performance thermoelectric materials[17,18], half-metallic magnetic semiconductors[19,20], and the recently predicted multifunctional topological insulators[21]. These compounds can offer a versatile range of relevant physical properties, i.e., they can have a vast variety of lattice constants and band gaps. Indeed, recent theoretical calculations[22] investigated a set of 648 hH compounds composed of group I, II, III, IV, and V elements of the periodic table, resulting in compounds I-I-VI, I-II-V, I-III-IV, II-II-IV, and II-III-III types, suggesting that there could be considerable flexibility in choosing materials over a substantial range of desired gap or lattice constant. Unfortunately, these hH materials were not yet systematically screened for PV applications as 1 eV and 1.7 eV band−gap materials lattice−matched to GaAs and Si, respectively. In this paper we propose five ternary hH compounds: ScAgC, YCuC, CaZnC, and NaAgO (LiCuS) as potential candidates for 1 eV (1.7 eV) band−gap materials matched to GaAs (Si) using first−principles total energy, band structure and lattice−dynamical calculations within the density functional theory. The paper is organized as follows: in section II, we briefly describe the computational techniques used in this work, results and

* abderrezak.belabbes@uni-jena.de

discussion will be presented in section III. We then end with some concluding remarks in section IV.

II. COMPUTATIONAL METHODS

Total energy calculations are performed using the full−potential linearized augmented plane wave (FP-LAPW) method as implemented in the WIEN2K code[24]. The exchange and correlation effects are treated within the generalized gradient approximation (GGA)[25]. Within the muffin−tin spheres we expand the set of basis functions up to R_{MT} K_{MAX} = 8 (R_{MT} is the muffin−tin radius, K_{MAX} is the maximum modulus of the reciprocal lattice vectors). The maximum value of partial waves inside an atomic sphere is l_{max} =10. The k−space integration on the Brillouin zone (BZ) for the self−consistent calculations is performed with a 14×14×14 k−point Monkhorst−Pack (MP) mesh[26]. The corresponding number of integration points in the irreducible part of the BZ amounts to 104 k−points. Spin is not taken into account. Since the number of valence electrons in the considered compounds is even, more precisely 18 (including the closed d shell of Cu or Ag), all spins of the electrons are paired. We made test calculations including the spin densities in collinear limit but also including spin−orbit interaction in the non−collinear limit. We always found vanishing magnetic moments. In the latter case both spin and orbital moments are zero in agreement with the so called "Slater−Pauling rules"[27,28] where the magnetic moment per formula unit is directly related to the number of valence electrons minus 18. This fact is in agreement with findings by Felser *et al.*[29,30], Galanakis *et al.*[19,31,32] and Offernes *et al.*[33]. The hH compounds have the general formula XYZ and crystallize in non−centrosymmetric cubic MgAgAs ($C1_b$) structure with the space group $F\bar{4}3m$ (space group no. 216). Also these compounds are called as Juza−Nowotny compounds which belong to the class of filled tetrahedral compounds[34]. A characteristic feature of this hH structure type are three interpenetrating fcc sublattices, each of which are occupied by the X, Y and Z atoms[35]. The corresponding occupied Wyckoff positions are 4a (0, 0, 0), 4b (1/2, 1/2, 1/2), and 4c (1/4, 1/4, 1/4).

Since the prediction of the correct gaps is essential, one has to take quasiparticle corrections into account to simulate the excitation effects[36]. We do it here in an approximate manner applying the Tran−Blaha method[37,38]. For the dynamical properties we apply again the GGA in a plane wave basis. We use ultrasoft Vanderbilt pseudopotentials[39] as implemented in the Quantum ESPRESSO package[40]. The electron wave functions are expanded in a plane−wave basis set up to a kinetic energy cutoff of 70 Ry, while an energy cutoff of 500 Ry is used for the charge density. The k−space integration of the BZ in the self−consistent calculations of densities and energies are performed with a 6 × 6 × 6 MP mesh. The lattice−dynamical properties are finally calculated using the density functional perturbation theory (DFTP)[41]. Here, a 4 × 4 × 4 q−point mesh of the MP type is used. The resulting matrices are then Fourier−interpolated to obtain complete phonon dispersion curves from their eigenvalues.

III. RESULTS AND DISCUSSION

A. Strategy

In order to identify a specialized class among the variety of 648 hH compounds studied previously by Gruhn[22], we systematically investigate them according to their physical properties using the following criteria: First, (i) since the hH geometry is quite similar to the common semiconductor zinc−blende structure as suggested in previous studies[34,42–46], we select materials which have a lattice parameter close to 5.65 Å and 5.43 Å for a good lattice matching with GaAs and Si, respectively. Note that the selected hH compounds with exceedingly small lattice mismatch possess many advantages over heterostructures with significantly strained interfaces, i.e., to guarantee high−quality, dislocation−free growth of such material combinations. Second, (ii) based on band gaps we only choose materials which have band gaps close to 1 eV (1.7 eV). Thereby, we restrict ourselves to direct gap materials because they are of most interest for optoelectronic applications. Moreover, deformation potentials of indirect materials are usually less well known. We should note that the structural defects, i.e., the presence of perturbations, such as lattice mismatch and strain effect, could play an important role in defining the band gap of the real hH/GaAs(Si) interfaces and their optical properties.

Based on these criteria, we identify five hH compounds as candidates that satisfy both conditions mentioned above. These compounds are ScAgC, YCuC, CaZnC, NaAgO, and LiCuS which are likely to be less explored among the possible hH compounds.[22] Interestingly, the list of selected candidates does not contain any toxic (Pb, Cd, As, Be) or expensive (Pd, Pt, Au, In) elements. Recently, a similar observation has been made for piezoelectric hH compounds by Roy *et al.*[47], and for I-II-V systems by Kieven *et al.*[43].

B. Structure and stability

One critically important physical property as indicator of the feasibility of the synthesis of these materials is the formation of enthalpy ΔH, i.e., the energy needed to form a compound out of its elemental constituents in their standard form. The computed values of ΔH of the five considered materials are given in Table I. The calculated negative values of the formation enthalpy of ScAgC, YCuC, CaZnC, NaAgO, and LiCuS indicate that these compounds are at least metastable. Their growth

TABLE I. The calculated lattice parameter a, bulk modulus B, band gap E_g, branch−point energy E_{BP}, band discontinuities ΔE_c and ΔE_v, and formation enthalpy ΔH of the hH compounds ScAgC, YCuC, CaZnC, NaAgO and LiCuS.

Compound	a(Å)	B(GPA)	E_g(eV)	E_{BP}(eV)	E_v(eV)	E_c(eV)	ΔE_v(meV)	ΔE_c(meV)	ΔH(eV)
CaZnC	5.740, 5.745[a]	76.2	1.177	1.17	−1.17	0.000	−630	−874	−3.76
NaAgO	5.700, 5.695[a]	57.7	0.918	1.99	−1.99	−1.074	−1451	−1954	−3.55
ScAgC	5.600, 5.600[a]	128.4	1.183	0.10	−0.10	1.082	440	202	−5.43
YCuC	5.650, 5.660[a]	118.6	1.095	0.72	−0.72	0.375	−179	−505	−5.88
LiCuS	5.579, 5.594[a]	65.73	1.88, (2±0.1)[b]	1.31	−1.31	0.548	−1067	−372	−4.07

[a] FPLAPW-GGA from Ref. [22]
[b] Collection of experimental data in Ref. [23]

should be possible under standard growth conditions, e.g. typical temperatures.

The calculated total energies are fitted with the Murnaghan equation of state[48] to obtain the structural parameters. The calculated energetic, structural, and elastic parameters for ground state phases, namely the equilibrium lattice parameter a, and the bulk modulus B, are given in Table I, in addition to the enthalpy. Our results for the lattice parameters excellently agree with those of the previous first−principles calculations of Gruhn[22]. Furthermore, we note a small mismatch between the lattice constants of ScAgC, YCuC, CaZnC, NaAgO and GaAs ($\Delta a/a_{GaAs}$=0%, 0.9%, 1.6%, and 5% for ScAgC, YCuS, CaZnC, and NaAgO, respectively), while between the lattice constant of LiCuS and Si the corresponding value is $\Delta a/a_{Si}$=2%. Therefore, we can not only expect the pseudomorphically growth of these compounds on a GaAs (Si) substrate. This especially holds for the highly ordered Heusler alloys on GaAs. Indeed, ScAgC can be grown perfectly lattice−matched to the GaAs substrate since $\Delta a/a_{GaAs}$= 0%. This observation opens possibilities of making heterojunctions between various combinations of these systems. The development of optical, optoelectronic and photovoltaic devices showing novel functionalities is likely.

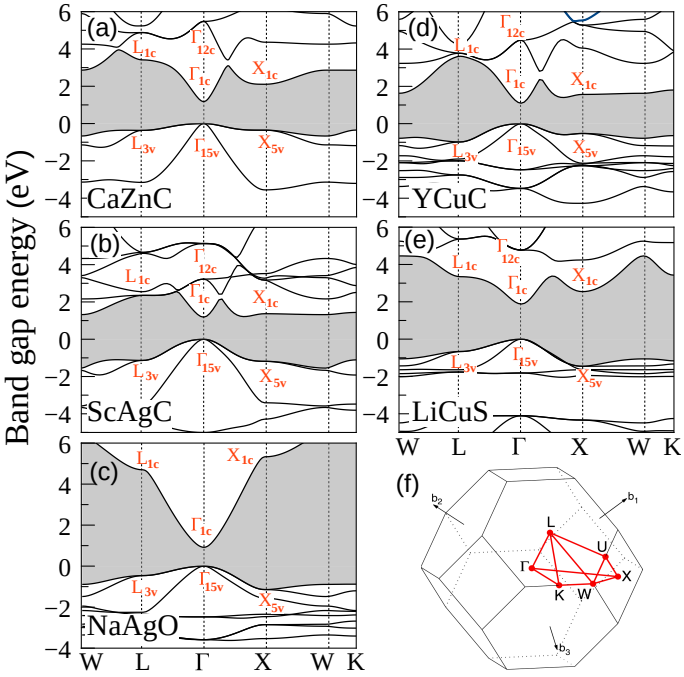

FIG. 1. (Color online) Band structure of the hH compounds CaZnC (a), ScAgC (b), NaAgO (c), YCuC (d), and LiCuS (e) with the associated BZ (f). The special points L, K, W, X, and the zone center Γ are highlighted.

C. Electronic structure

Because of the key importance of the band gaps, we use the modified Becke−Johnson (mBJ) exchange potential[37] within the GGA approximation, an approach that has been proved to yield band gaps in good agreement with experimental values for the majority of semiconductor materials[38,49]. This method competes in accuracy with expensive hybrid and GW[36,50,51]methods, and enables direct comparison with photoemission measurements. From a computational point of view, the calculation of a mBJ electronic structure is as fast as a conventional LDA calculation and hence demands much less computer resources than the GW method.

The electronic band structures along high−symmetry directions of the BZ are depicted in Fig. 1. The computed band gaps of the five hH systems under consideration are given in Table I. Based on the analysis of band structure calculated within GGA−mBJ, we found that these compounds possess direct band gaps with the transition $\Gamma_{15v} \rightarrow \Gamma_{1c}$. The energy gaps of ScAgC, YCuC, CaZnC, and NaAgO fail into the range of 0.91−1.18 eV, while the band gap of LiCuS is 1.88 eV. Since the gaps of the five hH compounds are direct, the characteristic band energies given in Fig. 1, especially those of the uppermost valence bands (VBs) at the Γ point, are most interesting for optoelectronic applications. This especially holds for the band ordering and the energy position of the conduction band minima at Γ, X, and L with respect to the valence band maximum (VBM) at Γ. Note that the energetical ordering in these hH compounds depends

sensitively on the actual atomic geometry and the strain state. This holds also for the band parabolicity and, in the worst case, the filling of the conduction band. Therefore, we did a careful symmetry analysis of the valence and conduction states at Γ to identify the band states which mainly consist of atomic $s-$, $p-$, or $d-$like orbitals. The resulting denotations are also presented in Fig. 1.

The parabola−shaped lowest conduction band exhibits a comparably strong dispersion and futures s character at Γ for all studied materials. In the case of the ScAgC and YCuC compounds a problem arises due to the relatively flat conduction bands along the BZ boundary along the XW and WK lines, which however are also not too far from the minimum near Γ. In contrast, NaAgO exhibits a strong dispersion of the conduction band minimum (CBM) near the BZ center with the energy at Γ being 4−5 eV lower than that in the outer regions of the BZ. This behavior is similar to other compounds with incorporated first−row elements like InN[52,53] or ZnO[54–57], which also show the strong dispersion and the nonparabolicity of the CBM. According to the symmetry analysis given in Fig. 1, the energetic ordering of the lowest conduction bands Γ_{1c} and Γ_{12c} is unique. They are well separated with the $d-$like Γ_{12c} level above the pure $s-$like Γ_{1c} one. This happens for all hH systems. The band ordering Γ_{12c}/Γ_{1c} and hence the band distance $\Delta_{\rm CB} = E_c(\Gamma_{1c}) - E_c(\Gamma_{12c})$ are clearly seen in Fig. 1. This band ordering is important because only optical transitions from the Γ_{15v} valence states into the Γ_{1c} conduction band states are essentially dipole−allowed. The same band ordering is found for other hH compounds with 8 or 18 valence electrons[21,33,58–60] which are likely to be semiconductors similar to the III-V systems[61–63]. The band structure details of the selected hH compounds are however more complex due to the hybridization of different atomic orbitals. This will discussed in detail in the next section.

Our calculations clearly indicate that the two fundamental requirements (i) and (ii) are fulfilled, i.e., the hH compounds ScAgC, YCuC, CaZnC, and NaAgO (LiCuS) are lattice−matched to GaAs (Si) with a direct band gap of ∼1 eV (1.7 eV).

Insight into the bonding interaction between constituents can be obtained from the site and orbital projected partial density of states (PDOS) analysis. Moreover, an analysis of the PDOS gives detailed information about the origin of CBM and VBM electronic energy levels. Such an analysis has been performed for all the hH compounds considered in the present work and is shown in Fig. 2. The top of valence bands is mainly due to the $2p-$C orbitals with relatively small contribution of $4d-$Ag and $3d-$Zn states for ScAgC and CaZnC, respectively, while the sub-valence band (−6.5 to −4 eV) contains a large contribution from the highly localized $3d-$Zn and $4d-$Ag states. However, for NaAgO and YCuC the strong coupling between the ($2p-$O $-4d-$Ag) and ($2p-$C $-3d-$Cu) states can be seen in the upper valence band with the d states more pronounced nearer the top of the valence band. Consequently the valence band is shifted toward higher energies due to reduced $p-d$ repulsion (see Fig. 2(c)(d)). For LiCuS, the lowest valence band (∼ −5 eV) is derived mainly from the hybridization of the $3p-$S and $3d-$Cu states. However, near the VBM roughly above −4 eV the $3d-$Cu orbitals are considerably stronger than the $3p-$S contribution. The smaller band gap in these hH compounds is mainly due to the fact that the $p-d$ interaction shifts the VBM $p-$bands closer to the CBM. The same effect is observed for Mg and Zn chalcogenides[64,65]. This finding is an important information concerning not only this class of hH compounds, but valid for all cases where localized d orbitals must be treated explicitly[66–70]. In the energy range of the CBM, on the other hand, unoccupied $3d-$Sc and $4d-$Y bands as well as states that show predominantly $s-$like symmetry at Γ can be found. The lowest conduction band is dispersive in the surroundings of the BZ center [Fig. 2(b)(d)]. This fact should be taken into consideration in the derivation of gaps from X−ray photoemission spectroscopy (XPS)/bremsstrahlung isochromat spectroscopy (BIS) spectra for ScAgC and YCuC, since the s states, due to their very low DOS in comparison to the d states, are almost invisible in BIS measurements.

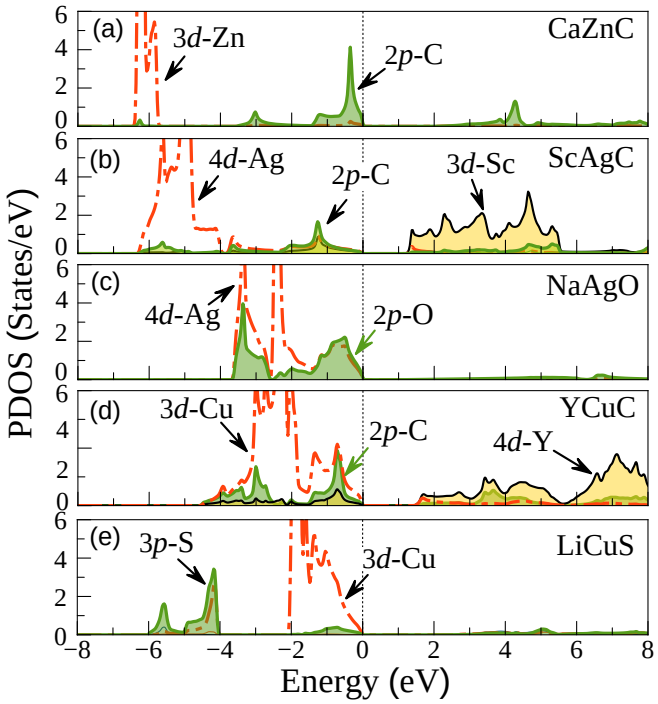

FIG. 2. (Color online) Projected density of states (PDOS) of the hH compounds CaZnC (a), ScAgC (b), NaAgO (c), YCuC (d) and LiCuS (e).

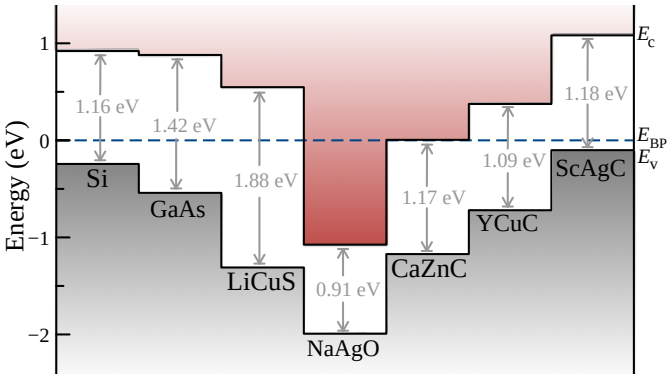

FIG. 3. (Color online) Conduction−band and valence−band edges for Si, GaAs, CaZnC, ScAgC, NaAgO, YCuC, and LiCuS compounds. The gray and red colored areas show the valence and conduction bands, respectively. They are aligned via the branch−point energy $E_{\rm BP}$. The calculated energies from Table I have been applied.

D. Band discontinuities

From the above results we can conclude that the mBJ functional reconciles not only the band gap but also the correct placement of all orbitals (coupling and admixture). Thus, we now proceed to further study the electronic properties of the hH compounds using the mBJ density-functional with confidence that this approach will provide a balanced and consistent description of their electronic structure.

Despite the fact that the heterointerfaces of Si or GaAs with hH compounds play an important role for the action of numerous devices, e.g. for the charge separation of optically excited electrons and holes in Si-based solar cells, practically nothing is known about these interfaces from a microscopic point of view. Therefore, knowledge about the interfaces of hH layers with GaAs or Si substrate is extremely important for the interpretation of experimental results and design of devices. The combination of the different hH compounds with GaAs(Si) substrates represents a heterostructure[71]. The questions arise how the electronic structures of these hH relate to each other and how the energy barriers for electrons and holes, i.e., the band discontinuities or band offsets, are formed. To answer to these questions an alignment of the energy scales of these materials is needed. For that reason we have to study the natural band discontinuities ΔE_c and ΔE_v.

In order to calculate the natural band offsets we use the branch−point energy $E_{\rm BP}$[57,72–75] as universal energy level of reference to align the energy bands of the studied hH compounds and GaAs(Si). The branch−point energy $E_{\rm BP}$ is calculated by a modification of the Tersoff method[72,73] as the mean value of the BZ averages of the topmost valence bands and the lowest conduction bands. The band structures used to compute $E_{\rm BP}$ have a strong relationship to surface states, so−called virtual gap states[76]. The charge neutrality level is identified as the level at which the surface states change from donor- to acceptor-like behavior. Therefore the surface Fermi level is pinned at this energy level, which can be exploited for band alignment. The used GGA-mBJ method leads to $E_{\rm BP}$ in close agreement with the more sophisticated Green-function[36,50] or HSE+GW methods[51] The positions of the BPEs with respect to the VBM together with the resulting natural band discontinuities ΔE_v and ΔE_c of the VBM and CBM, respectively, between the GaAs (Si) and hH materials computed within the GGA-mBJ approach[37] are also listed in Table I. They give rise to the band lineups as presented in Fig. 2. These band discontinuities are virtually unknown. Direct measurements of the band discontinuities of these hH have not yet been published.

A scaling of the band numbers according to the number of valence electrons without d electrons in the primitive unit cell is applied[57]. In the case of hH crystals we correspondingly include only the lowest CB s ($N_{\rm CB} = 1$) and the two uppermost VBs p ($N_{\rm VB} = 2$) over the entire BZ[57]. $N_{\rm CB}$ is clearly determined by the strong dispersion of the lowest CB near Γ in all cases, espcially for NaAgO. Regarding $N_{\rm VB}$, we exclude the third VB because it shows a much larger $\mathbf{k}$ dispersion throughout the BZ than the two uppermost ones.

As an interesting result we emphasize that for all of the studied materials, except NaAgO, $E_{\rm BP}$ lies below the CBM. We observe that $\Delta E_c < 0$ and $\Delta E_v > 0$, indicating staggered type−II heterojunctions. For the hH compounds the absolute positions of the band edges E_v and E_c using the $E_{\rm BP}$ alignment are rather different as shown in Fig. 2. This may be interpreted as a consequence of different CB and VB band dipersions. In the case of NaAgO we find $|\Delta E_c| > E_g$(Si). Therefore, this NaAgO−Si heterostructure even represents a misaligned type−III heterostructure, sometimes also called broken−gap heterostructure. Since this would imply that the lowest conduction−band states on the NaAgO side of the interface are energetically favored over the valence−band states in the GaAs or Si, we predict a charge transfer upon interface formation that should alter the interface dipole and shift the band edges toward a stable type−II junction. Since a real interface would inevitably possess an interface dipole, it is clear that the real band discontinuities of hH/GaAs(Si) heterostructures strongly depend on the interface structure and the electric interface dipole moment[77,78] induced by the charge transfer and related to the hybridization between the orbitals that control directly the sign and magnitude of the band discontinuities. Mönch[79] stated that the electric−dipole contribution can change the valence−band offsets in semiconductor heterostructures by up to 30% .

In the case of NaAgO, the level $E_{\rm BP}$ appears deep in the CB (see Fig. 2). The reason is the strong $\mathbf{k}$ dispersion of the lowest conduction band (see Fig. 1), which gives rise to an extremely low density of states near the

TABLE II. The calculated elastic constants C_{11}, C_{12}, and C_{44} as well as the bulk modulus B in GPa of the hH compounds ScAgC, YCuC, CaZnC, NaAgO and LiCuS.

Compound	C_{11}	C_{12}	C_{44}	B
CaZnC	241.2	5.4	31.8	84.0
NaAgO	108.7	32.2	6.6	57.7
ScAgC	233.5	63.4	43.5	120.1
YCuC	289.3	33.6	85.2	118.9
LiCuS	103.6	46.0	57.1	65.2

pronounced CBM and relatively large electron affinities (see Figs. 2 and 3). As a consequence, a surface n-accumulation layer should occur. Such a surface accumulation layer has been experimentally observed not only for oxides[80] but also for nitrides[81–83]. Different conclusions have been published with respect to the occurrence of surface electron accumulation[80,84] or surface electron depletion[85,86]. Nevertheless, in contrast to the majority of semiconductors and insulators there are strong theoretical and experimental arguments[57,61,80,84,87–90] that the branch points in the majority of oxides lie in the lowest conduction band and not in the fundamental gap. In any case, our prediction for $E_{\rm BP}$ is in agreement with the standard picture of studied oxides (see Ref. 57 and references therein).

E. Elastic and dynamical properties

The elastic constants of solids provide a link between mechanical and dynamical behaviors of crystals, and give important information concerning the nature of interatomic forces. In particular, they provide information on the local stability and stiffness of materials. The independent elastic constants C_{11}, C_{12}, and C_{44} calculated for single crystals are given in Table II. These elastic constants satisfy the requirements of mechanical stability for cubic crystal: $C_{11} - C_{12} > 0$, $C_{44} > 0$, $C_{11} - 2C_{12} > 0$. They clearly indicate that the predicted $C1_b$ phase of ScAgC, YCuC, CaZnC, NaAgO and LiCuS is a mechanically stable phase. It is also worth to note that the bulk modulus computed from the values of the elastic constants $B = (C_{11} + 2C_{12})/3$ is in good agreement with the one obtained through the fit of the Murnaghan equation of state (see Table II).

As a matter of fact, it is difficult to draw a conclusion about lattice stability of these compounds based only on elastic constants and formation enthalpies ΔH obtained from total energy calculations. Therefore, we also address the phonon properties in order to obtain a comprehensive picture of the dynamical stability of the equilibrium structure of the studied hH ScAgC, YCuC, CaZnC, NaAgO, and LiCuS compounds. It is a well established fact that the mechanic or thermodynamic stability only reflects the local stability of the crystal structure, while the full phonon dispersion curves are believed to shed light on the kinetic description and the structural stability of a compound.

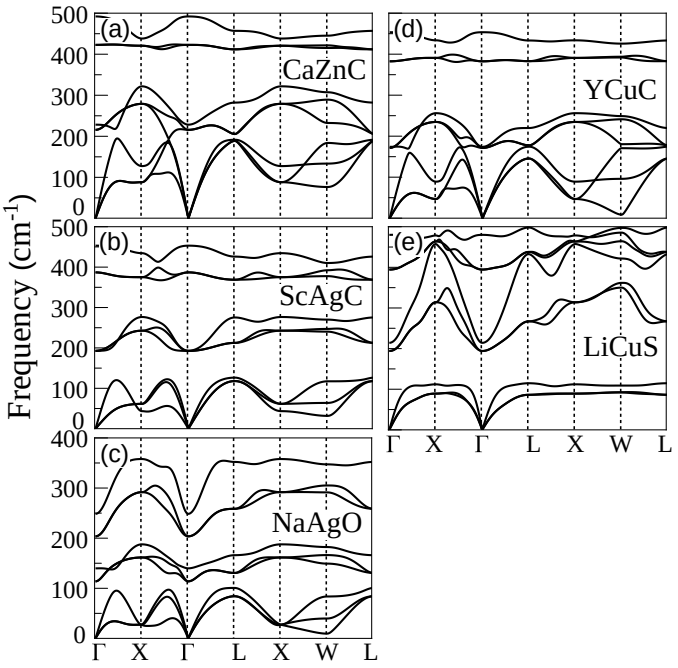

FIG. 4. (Color online) Phonon band structures of the hH compounds CaZnC (a), ScAgC (b), NaAgO (c), YCuC (d), and LiCuS (e).

The calculated phonon dispersion curves of the studied compounds along the high−symmetry lines of the BZ are displayed in Fig. 4. The three atoms in the primitive cell give rise to nine phonon branches, one longitudinal acoustic (LA), two transverse acoustic (TA), two longitudinal optical (LO), and four transverse optical (TO) branches. They show common features but also some differences in the spectra. First, the main difference between the spectra is the overlap between optical and acoustic modes in the case of YCuC and CaZnC, whereas for the other systems the modes are well separated by a large frequency gap despite the very large difference in atomic masses between the transition metals and the other atoms. This especially holds for LiCuS. This overlap effect is mainly related to the Born effective charge that splits the LO mode from the associated TO mode around Γ. The corresponding LO−TO splitting is characteristic for polar semiconductors and insulators[41].

For the investigated hH compounds this observation confirms the conclusion from the gaps in Table I that they are semiconductors. Indeed, like $A^{\rm III}B^{\rm V}$ semiconductors[41,91–94], the bonding in the hH compounds under consideration is determined by eight s and p electrons per unit cell which are expected to give rise to strong mixed ionic−covalent bonds as explained above. The phonon dispersion relations presented in Fig. 4 are

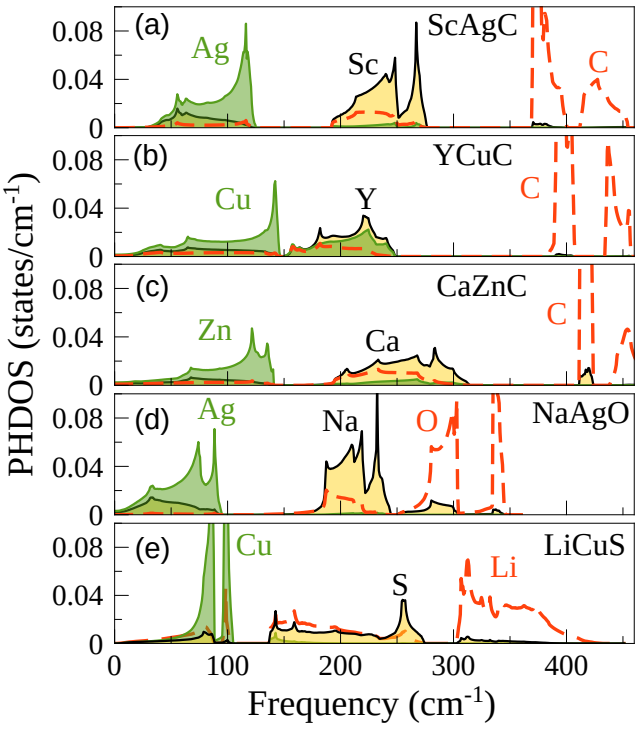

FIG. 5. (Color online) Partial phonon density of states (PHDOS) of the hH compounds ScAgC (a), YCuC (b), CaZnC (c), NaAgO (d), and LiCuS (e).

similar to those reported for other hH compounds such as ZrCoSb[95] and LiZnAs[96]. This may be interpreted as a further indication for the ability of DFPT and the good quality of the generated pseudopotentials[40].

There are three optical branches in the high−frequency region between 350 and 450 cm^{-1} in the phonon spectra as shown in Fig. 4. These phonon branches are less dispersive compared to the optical phonon branches in the lower frequency range. They are mainly dominated by the vibrations of C, O and Li atoms due to their lighter atom mass compared to the other two atoms. This can be seen more clearly from the partial phonon density of states in Fig. 5. For NaAgO and LiCuS, we find a pronounced dip in the dispersion of the LO branch at Γ. A similar behavior was observed in lead chalcogenides by Cardona *et al.*[97], Romero *et al.*[98], and Kilian *et al.*[99] who interpreted the LO dip as an indication for a "near Kohn anomaly".

The phonon branches in the lower frequency region exhibit considerable dispersion since the contribution of the heavier atoms is dominated at low frequencies (see Fig. 5). The only exception is LiCuS where the acoustic transverse and longitudinal branches (TA−LA) along the high symmetry directions are less dispersive than the optical phonon branches in the high frequency region. These acoustic branches (TA−LA) are very important to explain the relationship between the anomalous phonon dispersion and electron−phonon coupling. We notice that the acoustic branches do not possess any peculiarities and are similar to those for noble metals with fcc lattice which are not superconducting materials.

Most important, we clearly observe that calculated phonon band structure has no soft mode at any wave vector for all compounds, indicating thereby the dynamical stability of the studied hH systems. The phonon spectra of these hH systems in Fig. 4 and Fig. 5 are not studied experimentally and due to this circumstance the calculated spectra should be considered as a prediction.

IV. SUMMARY AND CONCLUSIONS

We have presented a detailed first−principles investigation of electronic, energetic, mechanical, and dynamical properties of hH semiconductors ScAgC, YCuC, CaZnC, NaAgO and LiCuS by using the full−potential linear augmented plane−wave, plane−wave pseudopotential methods and density functional linear−response theory. The direct band gaps of ScAgC, YCuC, CaZnC and NaAgO compounds are predicted to be in the range of 0.91−1.18 eV, while LiCuS is found to be wider−gap semiconductor with a direct band gap of 1.88 eV by the recently proposed modified Becke−Johnson exchange potential approximation. Moreover ScAgC, YCuC, CaZnC, NaAgO (LiCuS) compounds are found nearly lattice−matched to GaAs (Si). A tendency for misaligned type−II heterostructures is predicted for ScAgC, YCuC, CaZnC and LiCuS/GaAs(Si) which indicates highly efficient separation of electron−hole pairs generated at the GaAs (Si) side of a solar cell structure. In the NaAgO case even a tendency to a type−III heterostructure is visible. We also investigated the chances of synthesis of these compounds. The calculated formation enthalpies show thermodynamic stability, whereas the calculated elastic constants and phonon band structures show respectively mechanical and dynamical stability of these hH compounds. Therefore, we propose that ScAgC, YCuC, CaZnC, NaAgO and LiCuS could be strong candidates for photovoltaic applications in multi−junction devices.

[1] M. Kondow, K. Uomi, A. Niwa, T. Kitatani, S. Watahiki, and Y. Yazawa, Jap. J. Appl. Phys. **35**, 1273 (1996).
[2] J. S. Ng, W. M. Soong, M. J. Steer, M. Hopkinson, J. P. R. David, J. Chamings, S. J. Sweeney, and A. R. Adams, J. Appl. Phys. **101**, 064506 (2007).
[3] S. Tixier, S. E. Webster, E. C. Young, T. Tiedje, S. Fran-

coeur, A. Mascarenhas, P. Wei, and F. Schiettekatte, App. Phys. Lett. **86**, 112113 (2005).
[4] K. Nunna, S. Iyer, L. Wu, J. Li, S. Bharatan, X. Wei, R. T. Senger, and K. K. Bajaj, J. Appl. Phys. **102**, 053106 (2007).
[5] D. Reyes, D. Gonzalez, J. Ulloa, D. Sales, L. Dominguez, A. Mayoral, and A. Hierro, Nano. Res. Lett. **7**, 653 (2012).
[6] S. Almosni, C. Robert, T. Nguyen Thanh, C. Cornet, A. Ltoublon, T. Quinci, C. Levallois, M. Perrin, J. Kuyyalil, L. Pedesseau, A. Balocchi, P. Barate, J. Even, J. M. Jancu, N. Bertru, X. Marie, O. Durand, and A. Le Corre, J. Appl. Phys. **113**, 169902 (2013).
[7] R. Kudrawiec, J. Appl. Phys. **105**, 063529 (2009).
[8] R. Kudrawiec, J. Appl. Phys. **101**, 116101 (2007).
[9] J. Vidal, S. Botti, P. Olsson, J.-F. Guillemoles, and L. Reining, Phys. Rev. Lett. **104**, 056401 (2010).
[10] D. O. Scanlon and A. Walsh, App. Phys. Lett. **100**, 251911 (2012).
[11] J. R. Lang, J. Faucher, S. Tomasulo, K. Nay Yaung, and M. Larry Lee, App. Phys. Lett. **103**, 092102 (2013).
[12] M. Ferhat and F. Bechstedt, Phys. Rev. B **65**, 075213 (2002).
[13] A. Belabbes, M. Ferhat, and A. Zaoui, App. Phys. Lett. **88**, 152109 (2006).
[14] S. Chen, X. G. Gong, A. Walsh, and S.-H. Wei, App. Phys. Lett. **94**, 041903 (2009).
[15] Q. Shu, J.-H. Yang, S. Chen, B. Huang, H. Xiang, X.-G. Gong, and S.-H. Wei, Phys. Rev. B **87**, 115208 (2013).
[16] V. R. D'Costa, Y.-Y. Fang, J. Tolle, J. Kouvetakis, and J. Menéndez, Phys. Rev. Lett. **102**, 107403 (2009).
[17] J. Schmitt, Z. M. Gibbs, G. J. Snyder, and C. Felser, Mater. Horiz. **2**, 68 (2015).
[18] C. Uher, J. Yang, S. Hu, D. T. Morelli, and G. P. Meisner, Phys. Rev. B **59**, 8615 (1999).
[19] I. Galanakis, E. Şaşıoğlu, S. Blügel, and K. Özdoğan, Phys. Rev. B **90**, 064408 (2014).
[20] S. Ouardi, G. H. Fecher, B. Balke, X. Kozina, G. Stryganyuk, C. Felser, S. Lowitzer, D. Ködderitzsch, H. Ebert, and E. Ikenaga, Phys. Rev. B **82**, 085108 (2010).
[21] S. Chadov, X. Qi, J. Kübler, G. H. Fecher, C. Felser, and S. C. Zhang, Nat. Mater. **9**, 541 (2010).
[22] T. Gruhn, Phys. Rev. B **82**, 125210 (2010).
[23] D. Kieven, A. Grimm, A. Beleanu, C. Blum, J. Schmidt, T. Rissom, I. Lauermann, T. Gruhn, C. Felser, and R. Klenk, Thin Solid Films **519**, 1866 (2011).
[24] P. Blaha, K. Schwarz, G. K. H. Madsen, D. Kvasnicka, and J. Luitz, WIEN2k,*an augmented plane wave program for Calculating crystal properties* (Vienna University of Technology, Vienna, Austria (2001)).
[25] J. P. Perdew, K. Burke, and M. Ernzerhof, Phys. Rev. Lett. **77**, 3865 (1996).
[26] H. J. Monkhorst and J. D. Pack, Phys. Rev. B **13**, 5188 (1976).
[27] J. C. Slater, Phys. Rev. **49**, 931 (1936).
[28] L. Pauling, Phys. Rev. **54**, 899 (1938).
[29] C. Felser, L. Wollmann, S. Chadov, G. H. Fecher, and S. S. P. Parkin, APL Materials **3**, 041518 (2015).
[30] C. Felser, G. H. Fecher, and B. Balke, Ang. Chem. Int. Ed. **46**, 668 (2007).
[31] I. Galanakis, P. H. Dederichs, and N. Papanikolaou, Phys. Rev. B **66**, 134428 (2002).
[32] I. Galanakis, P. H. Dederichs, and N. Papanikolaou, Phys. Rev. B **66**, 174429 (2002).
[33] L. Offernes, P. Ravindran, and A. Kjekshus, J. Alloys Compd. **439**, 37 (2007).
[34] A. E. Carlsson, A. Zunger, and D. M. Wood, Phys. Rev. B **32**, 1386 (1985).
[35] P. J. Webster and K. R. A. Ziebeck, Vol. 19C (Landolt-Börnstein group III condensed matter, Berlin, 1988) pp. 75–184.
[36] F. Bechstedt, *Many-Body Approach to Electronic Excitations: Concepts and Applications* (Springer-Verlag, Berlin, Jena, 2014).
[37] F. Tran and P. Blaha, Phys. Rev. Lett. **102**, 226401 (2009).
[38] D. Koller, F. Tran, and P. Blaha, Phys. Rev. B **83**, 195134 (2011).
[39] D. Vanderbilt, Phys. Rev. B **32**, 8412 (1985).
[40] P. Giannozzi, S. Baroni, N. Bonini, M. Calandra, R. Car, C. Cavazzoni, D. Ceresoli, G. L. Chiarotti, M. Cococcioni, I. Dabo, A. Dal Corso, S. de Gironcoli, S. Fabris, G. Fratesi, R. Gebauer, U. Gerstmann, C. Gougoussis, A. Kokalj, M. Lazzeri, L. Martin-Samos, N. Marzari, F. Mauri, R. Mazzarello, S. Paolini, A. Pasquarello, L. Paulatto, C. Sbraccia, S. Scandolo, G. Sclauzero, A. P. Seitsonen, A. Smogunov, P. Umari, and R. M. Wentzcovitch, J. Phys. Condens. Matter **21**, 395502 (2009).
[41] S. Baroni, S. de Gironcoli, A. Dal Corso, and P. Giannozzi, Rev. Mod. Phys. **73**, 515 (2001).
[42] K. Kuriyama and T. Katoh, Phys. Rev. B **37**, 7140 (1988).
[43] D. Kieven, R. Klenk, S. Naghavi, C. Felser, and T. Gruhn, Phys. Rev. B **81**, 075208 (2010).
[44] D. M. Wood, A. Zunger, and R. de Groot, Phys. Rev. B **31**, 2570 (1985).
[45] T. Graf, C. Felser, and S. S. P. Parkin, Prog. Sol. St. Chem. **39**, 1 (2011).
[46] X. Zhang, L. Yu, A. Zakutayev, and A. Zunger, Adv. Funct. Mater. **22**, 1425 (2012).
[47] A. Roy, J. Bennett, K. Rabe, and D. Vanderbilt, Phys. Rev. Lett. **109**, 037602 (2012).
[48] F. D. Murnaghan, Proceedings of the National Academy of Sciences **30**, 244 (1944).
[49] J. A. Camargo-Martínez and R. Baquero, Phys. Rev. B **86**, 195106 (2012).
[50] L. Hedin, Phys. Rev. **139**, A796 (1965).
[51] J. Heyd, G. E. Scuseria, and M. Ernzerhof, J. Chem. Phys. **118**, 8207 (2003).
[52] A. Belabbes, J. Furthmüller, and F. Bechstedt, Phys. Rev. B **84**, 205304 (2011).
[53] J. Furthmüller, P. H. Hahn, F. Fuchs, and F. Bechstedt, Phys. Rev. B **72**, 205106 (2005).
[54] B.-C. Shih, Y. Xue, P. Zhang, M. L. Cohen, and S. G. Louie, Phys. Rev. Lett. **105**, 146401 (2010).
[55] W. R. L. Lambrecht, A. V. Rodina, S. Limpijumnong, B. Segall, and B. K. Meyer, Phys. Rev. B **65**, 075207 (2002).
[56] C. Friedrich, M. C. Müller, and S. Blügel, Phys. Rev. B **83**, 081101 (2011).
[57] A. Schleife, F. Fuchs, C. Rödl, J. Furthmüller, and F. Bechstedt, Appl. Phys. Lett. **94**, 012104 (2009).
[58] H. C. Kandpal, C. Felser, and R. Seshadri, Journal of Physics D: Applied Physics **39**, 776 (2006).
[59] S.-H. Wei and A. Zunger, Phys. Rev. Lett. **56**, 528 (1986).
[60] A. Walsh and S.-H. Wei, Phys. Rev. B **76**, 195208 (2007).
[61] F. Bechstedt and A. Belabbes, J. Phys.: Condens. Matter **25**, 273201 (2013).
[62] S. Assali, I. Zardo, S. Plissard, D. Kriegner, M. A. Verheijen, G. Bauer, A. Meijerink, A. Belabbes, F. Bechstedt,

J. E. M. Haverkort, and E. P. A. M. Bakkers, Nano Letters **13**, 1559 (2013).
[63] A. Belabbes, C. Panse, J. Furthmüller, and F. Bechstedt, Phys. Rev. B **86**, 075208 (2012).
[64] D. Segev and S.-H. Wei, Phys. Rev. B **68**, 165336 (2003).
[65] F. Boutaiba, A. Belabbes, M. Ferhat, and F. Bechstedt, Phys. Rev. B **89**, 245308 (2014).
[66] A. Schleife, F. Fuchs, J. Furthmüller, and F. Bechstedt, Phys. Rev. B **73**, 245212 (2006).
[67] M. Rohlfing, P. Krüger, and J. Pollmann, Phys. Rev. B **57**, 6485 (1998).
[68] S.-H. Wei and A. Zunger, Phys. Rev. B **37**, 8958 (1988).
[69] M. Shishkin and G. Kresse, Phys. Rev. B **75**, 235102 (2007).
[70] A. Fleszar and W. Hanke, Phys. Rev. B **71**, 045207 (2005).
[71] F. Bechstedt and P. Käckell, Phys. Rev. Lett. **75**, 2180 (1995).
[72] J. Tersoff, Phys. Rev. B **30**, 4874 (1984).
[73] J. Tersoff, Phys. Rev. B **32**, 6968 (1985).
[74] F. Flores and C. Tejedor, J. Phys. C Solid State **12**, 731 (1979).
[75] M. Cardona and N. E. Christensen, Phys. Rev. B **35**, 6182 (1987).
[76] W. Mönch, *Semiconductors Surfaces and Interfaces* (Springer, Berlin, 2001).
[77] W. R. L. Lambrecht and B. Segall, Phys. Rev. Lett. **61**, 1764 (1988).
[78] W. R. L. Lambrecht, B. Segall, and O. K. Andersen, Phys. Rev. B **41**, 2813 (1990).
[79] W. Mönch, App. Phys. Lett. **93**, 172118 (2008).
[80] P. D. C. King, T. D. Veal, D. J. Payne, A. Bourlange, R. G. Egdell, and C. F. McConville, Phys. Rev. Lett. **101**, 116808 (2008).
[81] I. Mahboob, T. D. Veal, L. F. J. Piper, C. F. McConville, H. Lu, W. J. Schaff, J. Furthmüller, and F. Bechstedt, Phys. Rev. B **69**, 201307 (2004).
[82] I. Mahboob, T. D. Veal, C. F. McConville, H. Lu, and W. J. Schaff, Phys. Rev. Lett. **92**, 036804 (2004).
[83] P. D. C. King, T. D. Veal, C. F. McConville, F. Fuchs, J. Furthmüller, F. Bechstedt, P. Schley, R. Goldhahn, J. Schrmann, D. J. As, K. Lischka, D. Muto, H. Naoi, Y. Nanishi, H. Lu, and W. J. Schaff, App. Phys. Lett. **91**, 092101 (2007).
[84] P. D. C. King, R. L. Lichti, Y. G. Celebi, J. M. Gil, R. C. Vilão, H. V. Alberto, J. Piroto Duarte, D. J. Payne, R. G. Egdell, I. McKenzie, C. F. McConville, S. F. J. Cox, and T. D. Veal, Phys. Rev. B **80**, 081201 (2009).
[85] A. Klein, App. Phys. Lett. **77**, 2009 (2000).
[86] C. Körder, P. Ágoston, and A. Klein, Sensors and Actuators B: Chemical **139**, 665 (2009).
[87] C. G. Van de Walle and J. Neugebauer, Nature **423**, 626 (2003).
[88] Y. Hinuma, A. Grüneis, G. Kresse, and F. Oba, Phys. Rev. B **90**, 155405 (2014).
[89] B. Höffling, A. Schleife, F. Fuchs, C. Rödl, and F. Bechstedt, App. Phys. Lett. **97**, 032116 (2010).
[90] B. Höffling, A. Schleife, C. Rödl, and F. Bechstedt, Phys. Rev. B **85**, 035305 (2012).
[91] J. A. Sanjurjo, E. López-Cruz, P. Vogl, and M. Cardona, Phys. Rev. B **28**, 4579 (1983).
[92] D. Touat, M. Ferhat, and A. Zaoui, J. Phys.: Condens. Matter **18**, 3647 (2006).
[93] J.-M. Wagner and F. Bechstedt, Phys. Rev. B **66**, 115202 (2002).
[94] A. Belabbes, A. Zaoui, and M. Ferhat, J. Phys.: Condens. Matter **20**, 415221 (2008).
[95] J. Shiomi, K. Esfarjani, and G. Chen, Phys. Rev. B **84**, 104302 (2011).
[96] D. M. Wood and W. H. Strohmayer, Phys. Rev. B **71**, 193201 (2005).
[97] M. Cardona, R. K. Kremer, R. Lauck, G. Siegle, J. Serrano, and A. H. Romero, Phys. Rev. B **76**, 075211 (2007).
[98] A. H. Romero, M. Cardona, R. K. Kremer, R. Lauck, G. Siegle, J. Serrano, and X. C. Gonze, Phys. Rev. B **78**, 224302 (2008).
[99] O. Kilian, G. Allan, and L. Wirtz, Phys. Rev. B **80**, 245208 (2009).